

Nuclear Spins as Quantum Memory in Semiconductor Nanostructures

W. M. Witzel and S. Das Sarma

*Condensed Matter Theory Center, Department of Physics,
University of Maryland, College Park, MD 20742-4111*

(Dated: January 24, 2020)

We theoretically consider the possibility of using solid state nuclear spins in a semiconductor nanostructure environment as long-lived quantum memory. In particular, we calculate, in the limit of a strong applied magnetic field, the quantum coherence time for P donor nuclear spins in random bath environments of Si and GaAs, and the lifetime of excited intrinsic spins in polarized Si and GaAs environments. In the former situation, the nuclear spin dephases due to spectral diffusion induced by the dipolar interaction among nuclei in the bath. We calculate this nuclear spin memory time in the context of Hahn and CPMG refocused spin echoes using a formally exact cluster expansion technique which has previously been successful in dealing with *electron* spin dephasing in a solid state nuclear spin bath. Although limited by the nuclear T_2 dephasing time, typically much shorter than its long-lived T_1 counterpart, we find that rather long nuclear spin quantum memory times of the order of 100 μ s (GaAs:P) and 1-2 ms (natural Si:P) are feasible using composite CPMG pulse sequences with the relative memory loss being less than 10^{-6} over these times scales. We also consider the complementary situation of a central flipped intrinsic nuclear spin in a bath of completely polarized nuclear spins where decoherence is caused by the direct flip-flop of the central spin with spins in the bath. Exact numerical calculations that include a sufficiently large neighborhood of surrounding nuclei show lifetimes on the order of 1-5 ms for both GaAs and natural Si. Our calculated nuclear spin coherence times may have significance for solid state quantum computer architectures using localized electron spins in semiconductors where nuclear spins have been proposed for quantum memory storage.

PACS numbers: 03.67.-a; 76.60.Lz; 03.65.Yz; 76.30.-v; 03.67.Lx

I. INTRODUCTION

The motivation for developing a solid state quantum computer architecture using localized spins as qubits arises primarily from the long presumed quantum coherence times for spins even in the strongly interacting solid state environment. In this respect, nuclear spins are ideal since both spin relaxation (i.e. T_1) and spin coherence (i.e. T_2) times are very long for nuclear spins, as compared with electron spins, due to their weak coupling to the environment. The application of a strong magnetic field further enhances nuclear coherence by suppressing, at least, the leading order relaxation and decoherence processes caused by direct hyperfine coupling between nuclear spins and any surrounding electron spins due to the large mismatch between electron and nuclear spin Zeeman energies. Throughout this paper we assume a strong applied magnetic field that defines the z -direction of our interacting spin system, and we also neglect, somewhat uncritically, all effects of any direct hyperfine coupling between electron spins and nuclear spins assuming our system to be entirely a nuclear spin system. The existence of localized electron spins in the environment will further suppress the nuclear spin coherence, and therefore, our theoretical values for nuclear spin quantum memory lifetimes should be taken as upper bounds.

The theoretical work presented in this article deals entirely with the quantum memory of nuclear spins in solid state spin quantum computer architectures. In particular, we directly calculate solid state nuclear spin decoherence in the nuclear spin bath environment, i.e.

for a Hamiltonian which contains *only* interaction between nuclear spins. Our work is of direct relevance to semiconductor-based quantum computer architectures where the idea of using nuclear spins to coherently store quantum spin memory has been seriously proposed in the literature.¹ As such, although we develop a rather general theoretical formalism for nuclear spin decoherence, we concentrate on GaAs quantum dots and phosphorus doped silicon, Si:P, for applying our theory since much of the solid state quantum computer work in the literature has focused on these two architectures. The theoretical question we address is simple and well-defined: How long is the solid state quantum memory time for nuclear spins in semiconductor structures? We answer this question in some detail for our specific model and systems, and discuss, using our formalism, how one can enhance the nuclear spin quantum memory (beyond the simple Hahn spin echo situation) by using composite pulse sequences to refocus nuclear spins. Our goal is thus a qualitative and quantitative understanding of nuclear spin quantum memory in GaAs quantum dots and Si:P doped structures taking into account the complex interacting environment of all the other nuclear spins invariably present in the solid state environment.

In considering nuclear spins as solid state quantum memory, we discuss two inequivalent (and perhaps complementary) situations. The usual situation is a bath of unpolarized nuclear spins surrounding the “central” donor nuclear spin which serves as our quantum memory. In this situation, spin relaxation processes (T_1) are suppressed by applying a strong magnetic field assuming

there is a significant mismatch between magnetic moments of the donor and intrinsic nuclei. Instead, the central spin memory dephases (T_2) primarily through the spectral diffusion mechanism that is induced by the surrounding nuclear spin bath. In the spectral diffusion process, which we consider first in section II, the central spin quantum memory is effectively subjected to a non-Markovian temporally fluctuating magnetic field due to the nuclear spin flip-flops in the surrounding bath that result from dipolar interactions among the bath nuclei. The spectral diffusion sets an ultimate limit to the coherence time for nuclear quantum memory storage in an unpolarized bath. There are, however, well-established procedures, going back fifty years, which can enhance (or more accurately restore) the quantum coherence over longer times. These coherence-enhancement protocols involve intricate refocusing of the nuclear spin dynamics through well-designed composite pulse sequences. We discuss a particular kind of coherence enhancement protocol, namely the Carr-Purcell-Meiboom-Gill (CPMG) composite pulse sequence, in the context of spectral diffusion induced nuclear spin memory decoherence in Sec. III of this article. In Sec. IV, we consider the complementary situation with quantum memory stored in a “central” intrinsic spin in a bath that is *completely* spin-polarized (perhaps through a dynamic nuclear polarization technique). This somewhat artificial situation (because complete nuclear spin polarization of the surrounding bath is highly improbable) is instructive because spectral diffusion is, by design, completely suppressed in a fully spin polarized nuclear spin bath (having no spin degrees of freedom available to cause fluctuations); relaxation, however, is now possible via direct dipolar flip-flops between the central nucleus and like nuclei (those with the same magnetic moment as the central nucleus and are thus still allowed to flip-flop in the limit of a strong applied magnetic field) in the bath. We solve this problem with exact quantum simulation (greatly simplified because of the complete polarization of the bath) and discuss the results in Sec. IV. We conclude in Sec. V with a discussion of the implications of our results for the solid state quantum information processing and of the various limitations of our theory.

II. SPECTRAL DIFFUSION OF A DONOR NUCLEUS

Nuclear storage of quantum information in a solid state environment is most naturally placed on donor nuclei that are easily distinguishable from the surrounding intrinsic nuclei. We note that it is imperative that the memory is stored in a nucleus which is distinct from the surrounding nuclei in some manner so that the stored information can be recovered. Several quantum computing architecture proposals¹ exploit the long-term quantum information storage capabilities which donor nuclei spins can possess. In this section, we present theoretical calcu-

lations of the T_2 dephasing of donor nuclear spins in two solid state environments of interest for quantum computing: Si:P and GaAs:P. Specifically, we present coherence versus time information in the context of simple Hahn echo refocusing; in the next section, we address multiple pulse Carr-Purcell-Meiboom-Gill (CPMG) refocusing.

We have previously reported² on a cluster expansion technique that is often applicable to spectral diffusion problems, giving formally exact solutions for short times. In some systems, formally exact solutions are obtained out to times that are longer than the decay-time of the system; in such cases, the cluster expansion method solves the entire problem for practical purposes because the tail of the decay is of no consequence (assuming a monotonic decrease in coherence with time). Other systems, including the donor nucleus spin decay currently being investigated, yield convergent cluster expansion results for only the initial part of the decay. For this reason, we focus on the initial decay and our plots show memory-loss as a function of time rather than exhibiting full, formally exact, decay curves.

In our model, we take the limit of a strong applied magnetic field which completely suppresses any interactions that do not conserve Zeeman energy. For simplicity, we also disregard interactions with any electrons; our Hamiltonian is solely composed of interactions between nuclei. We consider only the spectral diffusion decoherence mechanism due to the dipolar flip-flops in the nuclear bath surrounding the central nuclear spin. The bath Hamiltonian simply consists of dipolar flip-flop interactions between like nuclei:

$$\mathcal{H}_B \approx \sum_{n \neq m} \begin{cases} b_{nm} I_{n+} I_{m-} & , \text{if } \gamma_n = \gamma_m \\ 0 & , \text{otherwise} \end{cases} \quad (1)$$

$$b_{nm} = -\frac{1}{4} \gamma_n \gamma_m \hbar \frac{1 - 3 \cos^2 \theta_{nm}}{R_{nm}^3}. \quad (2)$$

Here, $I_{n\pm}$ denote the raising/lowering operator for the n^{th} nuclear spin and γ_n its gyromagnetic ratio, R_{nm} denotes the distance between nucleus n and m and θ_{nm} the angle of the vector between them relative to the applied magnetic field. Flip-flop interactions between unlike spins are suppressed via energy conservation due to the applied magnetic field. There is an additional $I_{nz} I_{mz}$ term which we find to have a negligible impact upon echo decay (we have performed calculations with and without this additional term).

The qubit-bath interactions are also due to dipolar coupling. (We refer to the central spin as a qubit to distinguish it from the nuclear spin bath.) However, in this instance we disregard the flip-flop interactions which are suppressed via energy conservation as a result of the applied magnetic field and differing gyromagnetic ratios between the qubit and spins in the bath. Instead, we consider just the $I_{nz} I_{mz}$ term which will contribute to

dephasing:

$$\mathcal{H}_A \approx \sum_n A_n I_{nz} S_z \quad (3)$$

$$A_n = \gamma_D \gamma_n \hbar \frac{1 - 3 \cos^2 \theta_n}{R_n^3}, \quad (4)$$

where S_z is a nuclear spin operator for the P donor nucleus, γ_D is the gyromagnetic ratio of the donor nucleus, R_n is the distance of nucleus n for the P donor, and θ_n is the angle of the vector from the P donor to nucleus n relative to the applied magnetic field.

The free evolution Hamiltonian is given by $\mathcal{H}_A + \mathcal{H}_B$. We represent the Hahn echo sequence by $\tau \rightarrow \pi \rightarrow \tau$ which we take to mean: free evolution for a time τ followed by a NMR π -pulse rotation about an axis perpendicular to the magnetic field, and then free evolution for another τ in time. The total echo time is $t = 2\tau$. Assuming complete disorder of the nuclear spins in the bath, expected in the large nuclear temperature limit ($T \gg nK$) without dynamic nuclear polarization or some such technique to generate order, the exact Hahn echo envelope (a measure of qubit coherence after performing the Hahn echo sequence) may be written:²

$$v_{\text{Hahn}}(\tau) = \frac{|\text{Tr} \left\{ U_+(\tau) U_-(\tau) U_+^\dagger(\tau) U_-^\dagger(\tau) \right\}|}{M}, \quad (5)$$

where M is the number of nuclear states and we define

$$\mathcal{H}_\pm = \mathcal{H}_B \pm \frac{1}{2} \sum_n A_n I_{nz}, \quad (6)$$

$$U_\pm(t) = e^{-i\mathcal{H}_\pm t}. \quad (7)$$

Using the formalism that we have laid out in Ref. 2, we can expand Eq. (5) in a way that includes contributions from “clusters” of successively increasing size. Defining $v_{\mathcal{C}}(\tau)$ as the solution to $v_{\text{Hahn}}(\tau)$ [Eq. (5)] when only considering those nuclei in some cluster (set) \mathcal{C} , a “cluster contribution” is recursively defined and computed by²

$$v'_{\mathcal{C}}(\tau) = v_{\mathcal{C}}(\tau) - \sum_{\substack{\{\mathcal{C}_i\} \text{ disjoint,} \\ \mathcal{C}_i \neq \emptyset, \mathcal{C}_i \subset \mathcal{C}}} \prod_i v'_{\mathcal{C}_i}(\tau), \quad (8)$$

subtracting from $v_{\mathcal{C}}(\tau)$ the sum of all products of contributions from disjoint sets of clusters contained in \mathcal{C} . Defined in this way, a cluster contribution can only be significant when interactions between nuclei in the set are significant and no part is isolated from the rest. We consider only local dipolar interactions in the current work, and thus contributions only arise when the nuclei in the set are spatially clustered together; hence we refer to these sets as clusters. The k th order of the cluster expansion for the echo [Eq. (5)] is then²

$$v^{(k)}(\tau) = \sum_{\substack{\{\mathcal{C}_i\} \text{ disjoint,} \\ \mathcal{C}_i \neq \emptyset, |\mathcal{C}_i| \leq k}} \prod_i v'_{\mathcal{C}_i}(\tau), \quad (9)$$

and involves clusters of size no larger than k . To simplify the calculation, the logarithm of the echo may be approximated as

$$\ln(v^{(k)}(\tau)) \approx \sum_{|\mathcal{C}| \leq k} v'_{\mathcal{C}}(\tau), \quad (10)$$

and corrections to this approximation, discussed in Ref. 2, may be computed to test its accuracy.

We have performed such cluster expansion calculations to successively approximate Eq. (5) for two different systems. In both systems, we have a P donor atom with $\gamma_D = \gamma_P = 1.08 \times 10^4 (\text{s G})^{-1}$, and we have chosen the applied magnetic field to point along one of the conventional axes directions (e.g., $B \parallel [001]$). In our figures, we plot “memory loss” versus total echo time (2τ) where we define memory loss as one minus the echo envelope, $1 - v_{\text{Hahn}}(\tau)$, and we only show results where the cluster expansion is rapidly convergent and the estimated correction to Eq. (10) is negligible. We show Hahn echo results (as well as CPMG results which will be discussed in the next section) for GaAs:P in Fig. 1; in this system, $\gamma_n = 4.58, 8.16, 6.42 \times 10^3 (\text{s G})^{-1}$ for ^{75}As , ^{71}Ga , and ^{69}Ga , respectively, and all differ from γ_P . We additionally show Hahn echo results (and CPMG results) for Si:P in Figs. 2 and 3; $\gamma_n = 5.31 \times 10^3 (\text{s G})^{-1}$ for ^{29}Si which also differs from γ_P . Unlike GaAs, Si has stable isotopes (^{28}Si , ^{30}Si) with zero spin. Among its stable isotopes, only ^{29}Si , which has a natural abundance of 4.67% and a spin of $1/2$, has a non-zero spin. Isotopic purification can reduce the amount of ^{29}Si and thereby diminish spectral diffusion caused by the nuclear spin bath. For generality, we define f to be the fraction of Si that is the ^{29}Si isotope. Figure 2 shows results in a natural Si bath ($f = 0.0467$), while Fig. 3 shows, for comparison, results in a bath of Si isotopically purified to $f = 0.01$.

As an alternative to the cluster expansion, a lowest order expansion of $v_{\text{Hahn}}(\tau)$ [Eq. (5)] in τ reveals that $v_{\text{Hahn}}(\tau) = 1 - O(\tau^4)$, and this simple lowest order approximation compares favorably with our cluster expansion results where $v_{\text{Hahn}}(\tau) \ll 1$. We can be slightly more sophisticated with this small τ approximation by applying it within the context of the cluster expansion; noting that $v'_{\mathcal{C}}(\tau) = O(\tau^4)$, Eq. (10) implies that $v_{\text{Hahn}}(\tau) = \exp[-O(\tau^4)]$. As discussed in previous work,² convergence for large systems (i.e., a large bath) is attained in this way by embedding the τ expansion, which is not necessarily convergent for large systems, within the context of the cluster expansion.

In the lowest order τ approximation discussed above, the GaAs:P result becomes

$$\ln(v_{\text{Hahn}}(\tau)) \approx - \left(\frac{\tau}{260 \mu\text{s}} \right)^4. \quad (11)$$

The exact (convergent) results plotted in Fig. 1 do not visibly differ from Eq. 11; therefore, this time expansion approximation is valid in the region in which the cluster expansion converges. By applying this lowest order time

expansion approximation, as well as the lowest order in the cluster expansion itself (involving only pair contributions), the Si:P result becomes

$$\ln(v_{\text{Hahn}}(\tau)) \approx -f^2 \left(\frac{\tau}{1.05 \text{ ms}} \right)^4. \quad (12)$$

The f^2 dependence simply arises from the fact that, in this approximation, all contributions are from pairs of nuclei. Dotted lines in Figs. 2 and 3 show the lowest order approximation of Eq. (12) for the Hahn echo (as well as the lowest order approximation for the CPMG pulse sequence which will be discussed in the next section). The exact (convergent) results exhibit a slight disagreement with the lowest order approximation as the cluster expansion nears the point of its divergence.

In previous studies of electron spin dephasing^{2,3} we noted good convergence of the cluster expansion for the full decay of the echoes as a result of a particularly applicable inter-bath perturbation that treats the coupling between members of the bath as a perturbation in the Hamiltonian. In that situation, the hyperfine coupling between the electron and the nuclei was much stronger than the dipolar coupling among nuclei. In the case of nuclear spin dephasing, however, the coupling to our central nucleus is no stronger than the coupling between members of the bath. In fact, the effective smallness of τ (compared to the inverse energies of the problem) is apparently the only reason for any cluster expansion convergence in the current study. As a consequence, the cluster expansion convergence is only attainable for short times (small values of τ) as indicated in Figs. 1-3. However, we do obtain convergent and accurate results of the *initial* quantum memory loss in the duration of high fidelity qubit memory retention which is of greatest significance in the context of quantum computing.

III. MULTIPLE PULSE REFOCUSING

It is well known in the NMR community that multiple pulse sequences may be used to prolong qubit coherence for a much greater time than the simple Hahn echo sequence. The simplest of these multiple pulse sequences is known as the Carr-Purcell-Meiboom-Gill (CPMG)⁴ scheme in which the Hahn echo sequence is simply repeated: $(\tau \rightarrow \pi \rightarrow \tau)^n$. In our previous work³ on electron spin coherence in semiconductors, independently confirmed in Ref. 5, we report that low-order symmetry-related cancellations occur when an even number of CPMG pulses are applied; this leads to significantly longer coherence times of even-pulse CPMG echoes compared with the Hahn echo. Also, increasing the number of these pulses will increase the overall coherence time with the assumption that the applied pulses are ideal. Consistent with these previous findings, we find that donor nucleus coherence is significantly enhanced by applying a two-pulse CPMG relative to the single pulse Hahn refocusing, and further enhanced, in

overall coherence time, by applying a four-pulse CPMG sequence. We now consider the application of multiple pulse echo sequences in prolonging nuclear spin quantum memory in semiconductor quantum computer architectures.

If we apply 2ν CPMG pulses, $(\tau \rightarrow \pi \rightarrow \tau)^{2\nu}$, the total echo time for this is $t = 4\nu\tau$, and the exact echo envelope may be written³

$$v_{\text{CPMG}}(t) = \frac{|\text{Tr} \{ [U(2\tau)]^\nu U(\tau) [U^\dagger(2\tau)]^\nu U^\dagger(\tau) \}|}{M}, \quad (13)$$

where we define

$$U(t) = U_+(t)U_-(t), \quad (14)$$

and refer to the definitions given in Eqs. (7) and (6). The cluster expansion is performed as described in the previous section using Eqs. (8) and (10) with the only exception that $v_{\mathcal{C}}(\tau)$ should now represent the solution, while considering only the nuclei in cluster \mathcal{C} , to Eq. (13). We have performed these cluster expansion calculations to successively approximate Eq. (13) for the GaAs:P and Si:P systems. We again plot “memory loss” versus total echo time ($4\nu\tau$) where memory loss is defined as $1 - v_{\text{CPMG}}(\tau)$. Results for 2 and 4 pulses ($\nu = 1$ and 2 respectively) in the GaAs:P system are shown in Fig. 1 where they are compared with Hahn echo results. Similarly, results for the natural and isotopically purified Si:P systems are respectively shown in Figs. 2 and 3 where they are also compared with corresponding Hahn echo results. A spin coherence enhancement when applying two pulses versus one pulse (Hahn echo) is apparent in the plots for each of these systems.

As shown in Ref. 3, if we apply a lowest order time expansion *and* an inter-bath perturbation (with coupling between nuclei as a perturbation in the Hamiltonian) approximation in the cluster contribution terms that go into the cluster expansion calculation, we find that $v_{\text{CPMG}}(\tau) \sim \exp[-O(\nu^2\tau^6)] = \exp[-O(\nu^{-4}t^6)]$. In this lowest order approximation, the general GaAs:P result becomes

$$\begin{aligned} \ln(v_{\text{CPMG}}(\tau)) &\approx -\nu^2 \left(\frac{\tau}{195 \text{ }\mu\text{s}} \right)^6 \\ &= -\nu^{-4} \left(\frac{t}{780 \text{ }\mu\text{s}} \right)^6, \end{aligned} \quad (15)$$

as compared with $\ln(v_{\text{Hahn}}(\tau)) \approx -(t/520 \text{ }\mu\text{s})^4$ [Eq. (11) rewritten in terms of t]. The exact (convergent) results plotted in Fig. 1 do not visibly differ from Eq. (11); therefore, this approximation is valid in the region in which the cluster expansion converges. This short time approximation equation may serve as a useful educated guess (estimate) at times beyond cluster expansion convergence. If we do extrapolate Eq. (15) equations and define T_2 as the time in which the extrapolated echo reaches $1/e$, then we have $T_2 = \nu^{0.67} \times 780 \text{ }\mu\text{s}$ for even CPMG echoes. This gives a factor of 6.5 increase of nuclear spin coherence

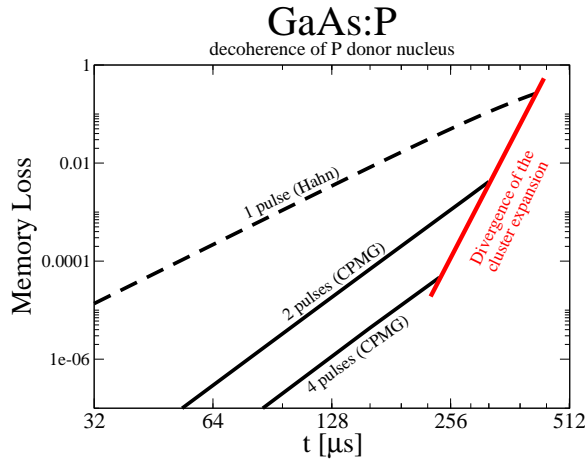


FIG. 1: Numerical results of nuclear spin quantum memory loss for a ^{31}P donor nucleus that replaces an As atom in bulk GaAs. We define memory loss as one minus the normalized echo and plot this in a log-log scale as a function of the total echo time. The dashed line gives the Hahn echo results and the solid lines give CPMG echo results for two and four pulses. At some point for each type of echo sequence, the cluster expansion fails to converge.

times relative to the electron spin quantum dot coherence times reported in Ref. 3. The behavior beyond the point of convergence may be an interesting theoretical question in itself. Are the curves well-behaved? Do they oscillate? Is it feasibly possible to obtain theoretical results in a regime in which cluster contributions *increase* with cluster size? These interesting and important questions are unfortunately beyond the scope of this work.

In the range of cluster convergence, where we have confidence in the accuracy of our results for the model that we have used, we observe high fidelity memory retention with a low loss of 10^{-6} up to $80 - 120 \mu\text{s}$ for two or four-pulse CPMG sequences. Increasing the number of CPMG pulses can improve fidelity versus time theoretically; however, in practice one will be limited by the finite time required to perform each π -pulse and by the accumulation of errors resulting from multiple pulses. Because our analysis assumes that each pulse is ideal, which is unlikely in practice, these theoretical results for T_2 should thus be regarded as an upper bound on the nuclear memory time.

Applying the lowest order approximation to the Si:P system, we similarly obtain

$$\begin{aligned} \ln(v_{\text{CPMG}}(\tau)) &\approx -\nu^2 f^2 \left[\left(\frac{\tau}{1.35 \text{ ms}} \right)^6 + f \left(\frac{\tau}{0.70 \text{ ms}} \right)^6 \right] \\ &= -\nu^{-4} f^2 \left(\frac{t}{5.4 \text{ ms}} \right)^6 \\ &\quad -\nu^{-4} f^3 \left(\frac{t}{2.8 \text{ ms}} \right)^6. \end{aligned} \quad (16)$$

as compared with $\ln(v_{\text{Hahn}}(\tau)) \approx -f^2(t/2.1 \text{ ms})^4$ [Eq. (12) rewritten in terms of t]. These lowest order

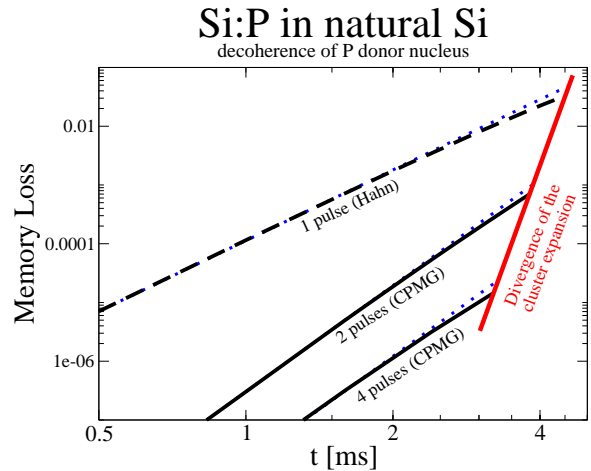


FIG. 2: Numerical results of nuclear spin quantum memory loss for a ^{31}P donor nucleus in bulk Si. We define memory loss as one minus the normalized echo and plot this in a log-log scale as a function of the total echo time. The dashed line gives the Hahn echo results and the solid lines give CPMG echo results for two and four pulses. Dotted lines give corresponding results, for comparison, obtained from the lowest order expansions provided by Eqs. (12) and (16). At some point for each type of echo sequence, the cluster expansion fails to converge.

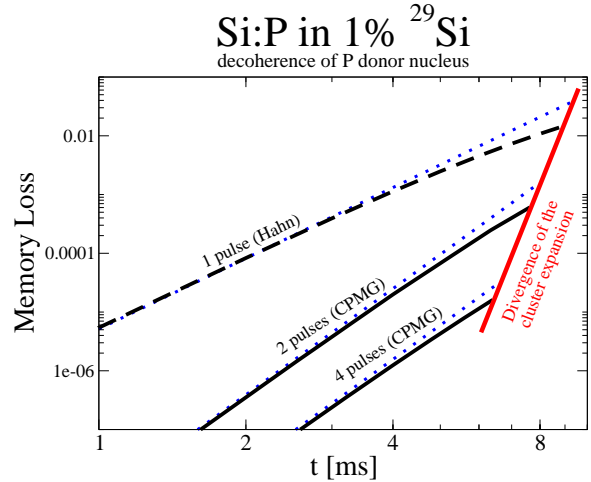


FIG. 3: Equivalent to Fig. 2 except that results are shown for Si purified to 1% ^{29}Si . Lowest order result given by Eqs. (12) and (16) are shown by the dotted lines. Isotopic purification enhances coherence as predicted in these equations.

results are shown as dotted lines in Figs. 2 and 3. The exact (convergent) results initially match this lowest order approximation, but show a slight disagreement as the cluster expansion nears the point of its divergence.

As with Eqs. (11) and (15), the above equations may serve as a useful educated guess (estimate) at times beyond cluster expansion convergence. Initially, at least, Figs. (2) and (3) show that Eqs. (12) and (16) provide conservative estimates. If we do extrapolate these equa-

tions and define T_2 as the time in which the extrapolated echo reaches $1/e$, then we have, for natural Si, $T_2 = \nu^{0.67} \times 12$ ms for even CPMG echoes. For a small number of pulses, $\nu \sim 1$, this gives about factor of 5 increase of nuclear spin coherence times relative to the electron spin quantum dot coherence times reported in Ref. 3; this comparison factor increases as we increase the number of pulses because electron spin decay-time³ scales with a smaller power of ν ($\nu^{0.53}$). In the range of cluster convergence, where we have confidence in the accuracy of our results for the model that we have used, we observe high fidelity memory retention with a low loss of 10^{-6} up to 1–2 ms for two or four-pulse CPMG sequences in natural Si and nearly up to 4 ms for 1% purified Si.

By implementing CPMG pulse sequences with just a few even number of pulses, high fidelity (with loss below 10^{-6}) qubit retention times are theoretically observed on the order of $100\ \mu\text{s}$ for GaAs systems and on the order of milliseconds for Si:P systems. We emphasize that although we are unable to achieve convergence beyond the initial decay (for reasons discussed at the end of section II) which affects the accuracy of our extrapolated estimate for T_2 , itself, we accurately estimate the initial-time coherent memory loss (i.e., the loss of the first 10^{-4} – 10^{-6} fraction of coherence) which is the most important ingredient for quantum computation considerations.

IV. INTRISIC SPIN RELAXATION

It has been proposed⁶ that quantum information could effectively be stored onto superpositions of coherent states of a nuclear spin ensemble, within a quantum dot for example, rather than addressing individual nuclei (such as donor nuclei). There are many practical considerations involved in determining the lifetime of such nuclear quantum memory storage in an actual nanostructure, including, for example interactions with an electron moved on or off of a quantum dot. Many of these considerations are implementation dependent, but any implementation will be subject to diffusion among nuclei. We consider the nuclear spin diffusion (or, more generally, spin transport) process in the simplest possible scenario of a completely polarized bath. The spectral diffusion induced by the nuclear bath is not possible in this scenario in the limit of a strong applied magnetic field because flip-flop processes cannot occur on their own in the polarized bath.

In this section, we study a well-defined and simple problem to compute the lifetime of quantum information stored in a central “intrinsic” (as opposed to a donor) nuclear spin, surrounded by a bath of fully polarized nuclei of the same type, and only considering nuclear spin degrees of freedom in the limit of a strong applied magnetic field. The precise scenario being considered here in the context of nuclear spin quantum memory lifetime is the following: The central spin in a polarized nuclear spin bath has its spin opposite to all the other spins in the

bath initially and we are interested in finding out how this local spin excitation moves (i.e., “diffuses”, although the process is technically not a diffusive process) away from the central spin due to dipolar coupling with surrounding nuclei. The central spin serves as the quantum memory which “decays” in time as the state evolves into a coherent superposition of excitation states involving spins in the bath. The effective Hamiltonian for the dipolar interaction, under the influence of a strong magnetic field which effectively conserves polarization via energy conservation, is given by

$$\mathcal{H} = \sum_{n \neq m} b_{nm} (I_{n+} I_{m-} - 2I_{nz} I_{mz}), \quad (17)$$

where the I_n operators operate on the nuclear spin at site n in the basis in which z is in the direction of the applied magnetic field. The dipolar coupling is given by

$$b_{nm} = -\frac{1}{4} \gamma_I^2 \hbar^2 \frac{1 - 3 \cos^2 \theta_{nm}}{R_{nm}^3}, \quad (18)$$

where θ_{nm} is the angle formed between the applied magnetic field and the bond vector linking the two spins. In a uniform applied magnetic field, which we assume, the total Zeeman energy will be constant when polarization is conserved. Therefore, the magnetic field does not affect the dynamics beyond determining the preferred z direction and justifying the polarization conservation approximation of Eq. (17).

In our initial state, we will assume a fully polarized nuclear spin bath. We denote the fully polarized state, including the polarization of the central spin, as $|\uparrow^N\rangle$. We denote the state with the spin of nucleus n lowered once (via the lowering spin operator) from its fully polarized state, but the remaining nuclei polarized, as $|n\rangle = I_{n-} |\uparrow^N\rangle$. We can store a qubit in the superposition of states $|\uparrow^N\rangle$ and $|0\rangle$. The state $|\uparrow^N\rangle$ is an eigenstate of Eq. (17) and is therefore stable. The $|0\rangle$ state, however, can decay as a result of a flip-flop with some neighboring nucleus; in this section, we will determine the lifetime of the $|0\rangle$ state for two different types of materials, GaAs and Si, and characterize the decay curve. We can solve this problem exactly by using a Hilbert space composed of the $|n\rangle$ states as a basis (since our Hamiltonian does not include any interactions that can take us out of this state-space). Conveniently, this state-space grows linearly with the number of nuclei (rather than the exponential growth of the Hilbert space that occurs in general) which allows this problem to be solved exactly even when there are many neighbors that influence the decay.

We wish to directly compute the probability that the system remains in state $|0\rangle$ after allowing the system to freely evolve for a time t :

$$P_0(t) = \|\langle 0 | \exp(-i\mathcal{H}t) | 0 \rangle\|^2. \quad (19)$$

To solve this problem directly, we first compute the matrix elements of \mathcal{H} in the $|n\rangle$ basis and then we can exponentiate this matrix via direct diagonalization. The

off-diagonal elements of \mathcal{H} are

$$\langle n | \mathcal{H} | m \rangle = 2Ib_{nm}, \forall n \neq m, \quad (20)$$

where I is the nuclear spin magnitude, assumed to be the same for all involved nuclei. To obtain this we have used

$$I_{\pm} |I, m\rangle = \sqrt{I(I+1) - m(m \pm 1)} |I, m \pm 1\rangle, \quad (21)$$

where only $I_+ |I, I-1\rangle$ and $I_- |I, I\rangle$ are relevant. We also have,

$$\langle n | \mathcal{H} | n \rangle = -2 \sum_{k \neq m} b_{km} I(I - \delta_{nk} - \delta_{nm}) \quad (22)$$

$$= -2 \sum_{k \neq m} b_{km} I^2 + 4 \sum_{m \neq n} b_{nm} I. \quad (23)$$

The first term in Eq. (23) is a constant contribution to the diagonal and therefore a constant, commuting contribution to the Hamiltonian that will not affect probabilities. We can therefore use an effective Hamiltonian, \mathcal{H}' , in which

$$\langle n | \mathcal{H}' | m \rangle = 2Ib_{nm}, \forall n \neq m, \quad (24)$$

$$\langle n | \mathcal{H}' | n \rangle = 4I \sum_{n \neq m} b_{nm}. \quad (25)$$

We may now solve the problem by successively including increasingly distant neighbors of the central spin into the simulated system until convergence is achieved. In a Bravais lattice with only one type of nucleus, $\langle n | \mathcal{H}' | n \rangle$ [Eq. (25)] is, by symmetry, a constant for all n and is therefore irrelevant (another constant energy in the system that plays no role in the dynamics). In lattices with mixed nuclei, this may not be completely irrelevant; however, we have performed calculations on real lattice systems with and without this part of the Hamiltonian finding that it has little effect on the results except that it artificially slows down the rate of convergence as we include increasingly distant neighbors (because it does lead to a significant finite size effect).

Calculated results are shown for pure ^{29}Si and natural Si in Figs. 4 and 5 respectively. The ^{29}Si has a spin of $1/2$ and $\gamma_I = 5.31 \times 10^3 \text{ (s G)}^{-1}$. The other stable isotopes of Si, ^{28}Si and ^{30}Si , have no net nuclear spin and therefore do not contribute to the decay. Si has a diamond lattice structure with a lattice constant of 5.43 \AA . In natural Si, there is a 4.67% abundance of ^{29}Si and the random placement of these nuclei leads to uncertainty in the results; the standard deviation is thus shown by the error bars in Fig. 5.

Calculated results are shown for GaAs in Fig. 6. There are three distinct problems with the central spin being ^{75}As , ^{69}Ga , or ^{71}Ga which have respective gyromagnetic ratios of $\gamma_I = 4.58, 6.42, 8.16 \times 10^3 \text{ (s G)}^{-1}$ and all have spins of $3/2$. The GaAs is in a Zincblende lattice structure with a lattice constant of 5.65 \AA . The ^{75}As occupies one fcc lattice while the ^{69}Ga and ^{71}Ga are randomly distributed in 60.4% and 39.6% respective concentrations on

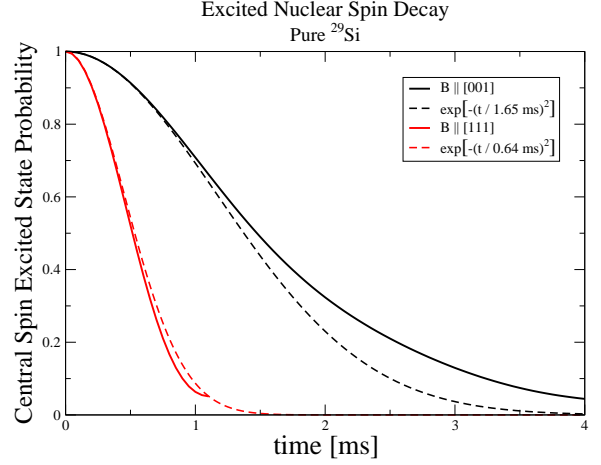


FIG. 4: Relaxation of a central ^{29}Si nuclear spin in a bath of polarized isotopically pure ^{29}Si nuclei in silicon's diamond lattice structure in the limit of a strong applied magnetic field along two directions with extremal results: B along [001] (or, equivalently, along any of the conventional axes, x , y , or z), and B along [111]. The dashed curves give the corresponding approximate solutions from Eq. (30).

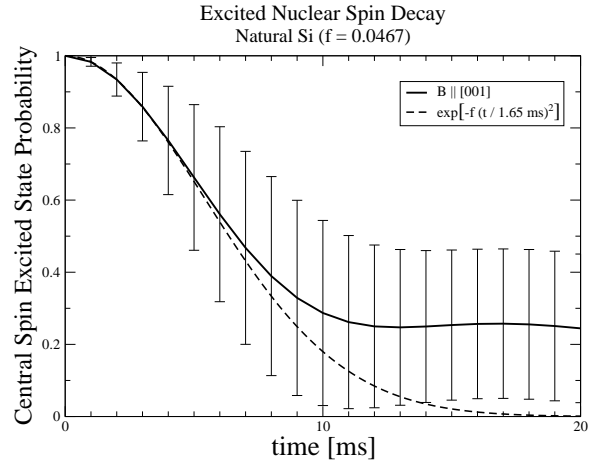


FIG. 5: Relaxation of a central ^{29}Si nuclear spin in a bath of polarized natural Si nuclei in silicon's diamond lattice structure in the limit of a strong applied magnetic field along one of the conventional axes (e.g., [100]). Error bars indicate the standard deviation as a result of random isotopic configurations ($4.67\% {^{29}\text{Si}}$ and the remaining ^{28}Si and ^{30}Si is spinless giving no contribution to the relaxation). The dashed curve gives the corresponding approximate solution from Eq. (30).

the other fcc lattice. The uncertainty in the random isotopic configuration of the Ga sublattice is the cause for standard deviations shown by the error bars in Fig. 6.

To approximate the short time behavior, let us first expand to the lowest order in powers of t . First note that $\langle 0 | \mathcal{H}' | 0 \rangle = 0$ so there is not a first power of t in the expansion. In order to obtain the next order (first

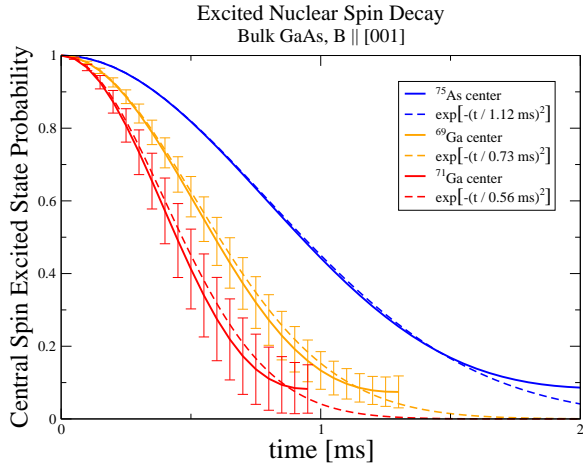


FIG. 6: Relaxation of a central ^{75}As , ^{69}Ga , or ^{71}Ga nuclear spin in a bath of polarized GaAs nuclei in GaAs's Zincblende lattice structure in the limit of a strong applied magnetic field along one of the conventional axes (e.g., [100]). In this limit, the central spin only interacts with like nuclei. The ^{75}As are arranged with certainty on one of the fcc lattices, while the ^{69}Ga and ^{71}Ga randomly occupy 60.4% and 39.6% of the other fcc lattice respectively. Error bars for the two Ga results indicate the standard deviation as a result of random isotopic configurations. The dashed curves give the corresponding approximate solutions from Eq. (30).

non-trivial order), we have

$$\langle 0 | (\mathcal{H}')^2 | 0 \rangle = \sum_n \langle 0 | \mathcal{H}' | n \rangle \langle n | \mathcal{H}' | 0 \rangle \quad (26)$$

$$= 4I^2 \sum_{n \neq 0} b_{n0}^2, \quad (27)$$

so then

$$\langle 0 | \exp(-i\mathcal{H}t) | 0 \rangle \approx 1 - 2I^2 \sum_{n \neq 0} b_{n0}^2 t^2. \quad (28)$$

Squaring this and keeping only terms up to t^2 , we finally obtain

$$P_0 \approx 1 - (2I)^2 \sum_{n \neq 0} b_{n0}^2 t^2. \quad (29)$$

To better match the shape of the decay curves, we use an exponential in time that is consistent with the above approximation:

$$P_0 \approx \exp \left(-f(2I)^2 \sum_{n \neq 0} b_{n0}^2 t^2 \right). \quad (30)$$

In order to effectively average over isotopic configurations, we have now explicitly inserted the dependence on the fraction, f , of nuclei in the lattice (or sublattice) that is of the same type as the central spin. This equation is indeed a good approximation to the initial decay and

is exhibited by the dashed curves in Figs. (4), (5), and (6). A good characterization of the lifetime is the time in which this approximation reaches $1/e$ which is given by

$$t_0 = 1 / \sqrt{f(2I)^2 \sum_{n \neq 0} b_{n0}^2}. \quad (31)$$

This also indicates how the lifetime scales with isotopic purification (e.g., in Si). Using this t_0 to define the lifetime, natural Si has a lifetime of 1.7 ms, and for GaAs, ^{75}As , ^{69}Ga , and ^{71}Ga have lifetimes of 1.1 ms, 0.7 ms, and 0.6 ms respectively. Note that while there is a greater abundance of ^{75}As than the other nuclear types in GaAs, it has a longer lifetime due to its relatively small gyromagnetic ratio.

V. CONCLUSION

We have analyzed in this work two complementary theoretical issues regarding the prospect for using nuclear spins in semiconductor materials, specifically GaAs and Si (with and without P doping), as long lived quantum memory, finding, in general that solid state nuclear quantum memory time could be one to two orders of magnitude longer than the corresponding electron spin coherence times. Thus, using nuclear spins as quantum memory in semiconductor nanostructures may be useful in the context of solid state quantum information processing architectures.

The two solid state nuclear spin coherence issues addressed in this article involve two complementary situations, both in the limit of a strong applied magnetic field: (1) quantum memory stored in a donor nuclear spin in a surrounding unpolarized nuclear spin bath where the main memory loss (i.e. decoherence) occurs through the spectral diffusion mechanism associated with the non-Markovian temporally fluctuating random magnetic field created by the dipolar flip-flops in the nuclear spin bath (sections II and III); (2) quantum memory stored in a central spin in a surrounding spin-polarized nuclear spin bath where spectral diffusion mechanism is suppressed, but spin memory relaxes through direct flip-flop interactions with neighboring like spins (section IV). While the physics associated with the two mechanisms is quite different, we find that quantum memory times of the order of 0.1 – 1 ms (1 – 10 ms) are quite feasible in GaAs (natural Si) using nuclear spin storage in each case. Still longer memory times may be achieved by using composite pulse sequences which can restore spin coherence, however, only at the considerable overhead of generating precise multiple pulse sequences. In Si, it is, in principle, possible to extend quantum memory time indefinitely through isotopic purification by eliminating all ^{29}Si nuclear since ^{28}Si and ^{30}Si nuclear have no free spin moments. The issue of reading and writing quantum memory on nuclear spins, obviously questions of great practical importance in the context of memory storage, are

not addressed at all in our work where we concentrate entirely on the theoretical evaluation of the nuclear spin quantum memory time itself assuming uncritically that memory reading and writing can be done without any loss or decay. Thus the lifetimes for nuclear spin quantum memory calculated in this work should be considered upper bound estimates in the context of realistic implementations. We conclude by pointing out that the coherence times we calculate in sections II and III of this

paper are essentially the nuclear T_2 dephasing time for the corresponding solid state environment, and as such our calculated T_2 values (~ 0.1 ms in GaAs, ~ 1 ms in Si) are in reasonable agreement with the existing solid state NMR literature⁷ on nuclear spin coherence in semiconductors.

This work is supported by ARO-DTO, ARO-LPS, and NSA-LPS.

¹ B.E. Kane, *Nature* **393**, 133 (1998); A.J. Skinner, M.E. Davenport, B.E. Kane, *Phys. Rev. Lett.* **90**, 087901 (2003); Xuedong Hu and S. Das Sarma, *Phys. Stat. Sol. (b)* **238**, 260 (2003); S. Das Sarma *et al.*, *Solid State Communications* **133**, 737 (2005); R. de Sousa, cond-mat/0610716;

² W.M. Witzel, R. de Sousa, S. Das Sarma, *Phys. Rev. B* **72**, 161306(R) (2005); W.M. Witzel and S. Das Sarma, *Phys. Rev. B* **74**, 035322 (2006).

³ W.M. Witzel and S. Das Sarma, cond-mat/0604577.

⁴ The Carr Purcell pulse sequence is arguably a more simple sequence than CPMG, but they differ only in the initialization pulse for experimental measurements in bulk that is irrelevant for our purposes. The CPMG sequence provides better protection against pulse errors for even echoes. Since we treat only even multiple-pulse echoes, showing them to

have improved coherence in the presence of the nuclear bath, we choose to refer to our considered multiple-pulse sequence as CPMG.

⁵ Wang Yao, Ren-Bao Liu, L.J. Sham, *Phys. Rev. B* **74**, 195301 (2006); Wang Yao, Ren-Bao Liu, L.J. Sham, cond-mat/0604634.

⁶ J.M. Taylor, C.M. Marcus, M.D. Lukin, *Phys. Rev. Lett.* **90**, 206803 (2003); Changxue Deng and Xuedong Hu, *IEEE Trans. Nano.* **4**, 35 (2005).

⁷ D. Paget *et al.*, *Phys. Rev. B* **15**, 5780 (1977); R. K. Hester *et al.*, *Phys. Rev. B* **10**, 4262 (1974); G.P. Carver, D.F. Holcomb, J.A. Kaeck, *Phys. Rev. B* **3**, 4285 (1971); R. K. Sundfors, *Phys. Rev.* **185**, 458 (1969); R. K. Sundfors and D. F. Holcomb, *Phys. Rev.* **136**, A810 (1964).